Journal of Biomolecular NMR, 7 (1996) 59–71
ESCOM

J-Bio NMR 320

Assignment of aliphatic side-chain ^1H_N / ^{15}N resonances in perdeuterated proteins

Bennett T. Farmer II[a,*] and Ronald A. Venters[b]

[a]*Bristol-Myers Squibb Pharmaceutical Research Institute, P.O. Box 4000, Princeton, NJ 08543-4000, U.S.A.*
[b]*Duke University NMR Center, Duke University Medical Center, P.O. Box 3711, Durham, NC 27710, U.S.A.*

Received 30 June 1995
Accepted 18 September 1995

Keywords: Perdeuteration; Side-chain ^1H_N / ^{15}N assignment; Human carbonic anhydrase II; 3D NMR

Summary

The perdeuteration of aliphatic sites in large proteins has been shown to greatly facilitate the process of sequential backbone and side-chain ^{13}C assignments and has also been utilized in obtaining long-range NOE distance restraints for structure calculations. To obtain the maximum information from a 4D $^{15}N/^{15}N$-separated NOESY, as many main-chain and side-chain ^1H_N / ^{15}N resonances as possible must be assigned. Traditionally, only backbone amide ^1H_N / ^{15}N resonances are assigned by correlation experiments, whereas slowly exchanging side-chain amide, amino, and guanidino protons are assigned by NOEs to side-chain aliphatic protons. In a perdeuterated protein, however, there is a minimal number of such protons. We have therefore developed several gradient-enhanced and sensitivity-enhanced pulse sequences, containing water-flipback pulses, to provide through-bond correlations of the aliphatic side-chain ^1H_N / ^{15}N resonances to side-chain ^{13}C resonances with high sensitivity: NH_2-filtered 2D ^1H-^{15}N HSQC (H_2N-HSQC), 3D $H_2N(CO)C_{\gamma/\beta}$ and 3D $H_2N(COC_{\gamma/\beta})C_{\beta/\alpha}$ for glutamine and asparagine side-chain amide groups; 2D refocused $H(N_{\varepsilon/\zeta})C_{\delta/\varepsilon}$ and $H(N_{\varepsilon/\zeta}C_{\delta/\varepsilon})C_{\gamma/\delta}$ for arginine side-chain amino groups and non-refocused versions for lysine side-chain amino groups; and 2D refocused $H(N_\varepsilon)C_\zeta$ and nonrefocused $H(N_{\varepsilon,\eta})C_\zeta$ for arginine side-chain guanidino groups. These pulse sequences have been applied to perdeuterated ^{13}C-/^{15}N-labeled human carbonic anhydrase II (^{2}H-HCA II). Because more than 95% of all side-chain ^{13}C resonances in ^{2}H-HCA II have already been assigned with the C(CC)(CO)NH experiment, the assignment of the side-chain ^1H_N / ^{15}N resonances has been straightforward using the pulse sequences mentioned above. The importance of assigning these side-chain H_N protons has been demonstrated by recent studies in which the calculation of protein global folds was simulated using only ^1H_N-^1H_N NOE restraints. In these studies, the inclusion of NOE restraints to side-chain H_N protons significantly improved the quality of the global fold that could be determined for a perdeuterated protein [R.A. Venters et al. (1995) *J. Am. Chem. Soc.*, **117**, 9592–9593].

Introduction

The perdeuteration of aliphatic proton sites has extended the application of triple-resonance NMR methodology to increasingly larger proteins (Grzesiek et al., 1993b; Yamazaki et al., 1994b). The determination of sequential backbone assignments (LeMaster and Richards, 1988; Torchia et al., 1988; Grzesiek et al., 1993b; Yamazaki et al., 1994b) and side-chain ^{13}C assignments (Farmer II and Venters, 1995) has benefited specifically from this isotopic labeling technique. Previously, deuteration to ~75% was demonstrated to enhance the intensity of ^1H_N-^1H_N NOE peaks by two- to threefold in large proteins (LeMaster and Richards, 1988; Torchia et al., 1988; Lemaster, 1990). Fractional deuteration was also exploited to reduce NOE spin diffusion in a general way (Torchia et al., 1988; Arrowsmith et al., 1990; Tsang et al., 1990; Reisman et al., 1991; LeMaster, 1994), thereby simplifying the extraction of distance restraints. Most recently, the potential to determine protein global folds using only ^1H_N-^1H_N NOE restraints derived from a perdeuterated protein has been explored (Venters et al.,

*To whom correspondence should be addressed.

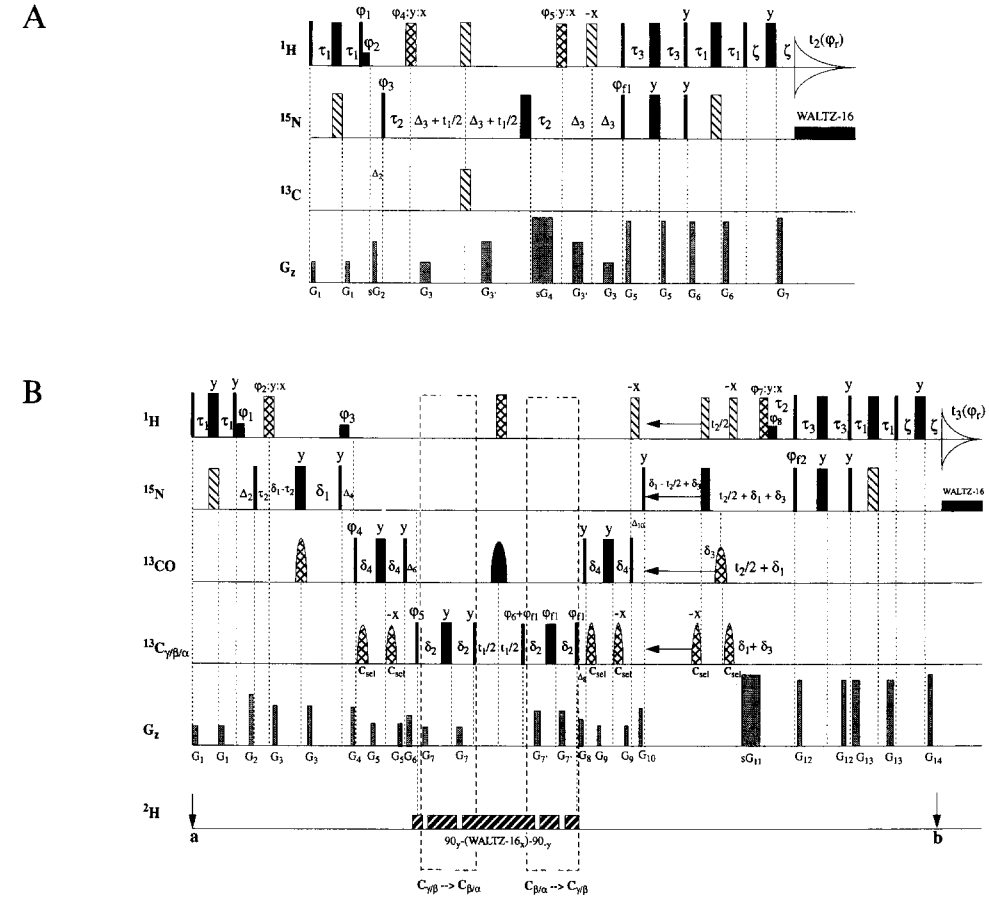

Fig. 1. Pulse sequences used to assign the aliphatic side-chain ^1H_N / ^{15}N resonances in perdeuterated ^{13}C-/^{15}N-labeled HCA II. In the sequences, 90° pulses are represented by wide lines, simple 180° pulses by black rectangles, and $90_x240_y90_x$ and $90_x180_y90_x$ composite inversion pulses (Levitt, 1986) by striped and cross-hatched rectangles, respectively. Cross-hatched ^1H pulses labeled $\varphi_{\#}$:y:x represent $90_{\varphi\#}180_y90_x$ rf pulse sandwiches. For $\varphi_{\#} = x$, this pulse sandwich acts as a composite 180° pulse; for $\varphi_{\#} = -x$, it acts as a composite 0° pulse. Gaussian- (solid black) and G3-shaped (cross-hatched) (Emsley and Bodenhausen, 1987) selective inversion pulses are drawn as bell-shaped pulses. In pulse sequences with ^2H decoupling, points **a** and **b** on the ^2H line indicate lock-holding/blanking and lock-unblanking/resampling, respectively. (A) The 2D NH_2-filtered ^1H-^{15}N gradient-enhanced, sensitivity-enhanced HSQC for identifying the side-chain amide ^1H_N / ^{15}N resonances of asparagine and glutamine residues with high sensitivity. The ^{13}C and ^{15}N carriers were set to 115.5 and 119.7 ppm, respectively. The water-selective 90° ^1H flipback pulse, labeled with phase φ_2, had a duration of 2.1 ms for $\varphi_1 = y$ and of 2.08 ms for $\varphi_1 = -y$. Phase-cycle elements were: $\varphi_1 = 8(y),8(-y)$; $\varphi_2 = 2(182°),4(2°),2(182°),2(167.5°),4(347.5°),2(167.5°)$; $\varphi_3 = x,-x$; $\varphi_4 = 2(x),2(-x)$; $\varphi_5 = 4(x),4(-x)$; and $\varphi_r = x,2(-x),x,-x,2(x),2(-x),2(x),-x,x,2(-x),x$. Additional rf acquisition parameters were: sw(^{15}N) = 2.04 kHz, sw(^1H) = 11.0 kHz, RD (relaxation delay) = 2.5 s, $t_1^{max} = 62.26$ ms, $t_2 = 70.0$ ms, $\tau_1 = 2.65$ ms, $\tau_2 = 5.56$ ms, $\tau_3 = 1.33$ ms, $\zeta = 1.2$ ms, and $\gamma B_2(^{15}N_{decouple}) = 1.27$ kHz with WALTZ-16 (Shaka et al., 1983). Gradient parameters were: $G_1 = -8$ G/cm, $t_{G1} = 0.3$ ms, $G_2 = -10$ G/cm, $t_{G2} = 1$ ms, $\Delta_2 = 2$ ms, $G_3 = -28$ G/cm, $t_{G3} = 0.25$ ms, $\Delta_3 = 0.3$ ms, $G_{3'} = -56$ G/cm, $t_{G3'} = 0.25$ ms, $G_4 = -32$ G/cm, $t_{G4} = 5.0$ ms, $G_5 = 32$ G/cm, $t_{G5} = 0.3$ ms, $G_6 = -32$ G/cm, $t_{G6} = 0.4$ ms, $G_7 = -32.03$ G/cm, and $t_{G7} = 0.5$ ms. Sixty-four transients were collected per FID for a total acquisition time of 12 h. (B) 3D $H_2N(CO)C_{\gamma/\beta}$ and $H_2N(COC_{\gamma/\beta})C_{\beta/\alpha}$ for assigning the side-chain amide ^1H_N / ^{15}N resonances of asparagine and glutamine residues. The ^{13}C and ^{15}N carriers were set to 36 and 110 ppm, respectively. All CO-selective pulses were frequency-shifted ~21 kHz to have a center excitation frequency at 175 ppm (Patt, 1992); only the Gaussian-shaped pulse at the center of the t_1 evolution period was cosine-modulated to eliminate Bloch–Siegert shifts on the precessing ^{13}C magnetization (McCoy and Mueller, 1992). CO-selective G3-shaped and Gaussian-shaped pulses had durations of 552 µs and 192 µs, respectively. CO-selective and $C_{\gamma/\beta/\alpha}$-selective 90° rectangular pulses had a duration of 44.7 µs; and 180° pulses of 40.6 µs. The C_{sel} inversion pulses ($^{13}C_{\gamma/\beta/\alpha}$ line) were G3-shaped, with a duration of 581 µs. The water-selective 90° ^1H flipback pulse labeled with phase φ_1 had a duration of 2.1 ms; and the 180° pulses labeled with phases φ_3 and φ_8 had a duration of 4.2 ms. For $\varphi_2 = x$ and $\varphi_7 = x$, the selective ^1H inversion pulses with phases φ_3 and φ_8, respectively, were applied; for $\varphi_2 = -x$ and $\varphi_7 = -x$, however, the same pulses were replaced by a delay of equivalent duration (4.2 ms). The t_1 evolution time was delayed by a half-dwell time (Bax et al., 1991) in both experiments. Common phase-cycle elements were: $\varphi_1 = 2°$; $\varphi_2 = 4(x),4(-x)$; $\varphi_3 = -x$; $\varphi_4 = x,-x$; $\varphi_6 = 2(-y),2(y)$; and $\varphi_7 = 8(x),8(-x)$. Specific phase-cycle elements for the $H_2N(CO)C_{\gamma/\beta}$ experiment were: $\varphi_5 = x$, and $\varphi_r = x,2(-x),x,-x,2(x),2(-x),2(x),-x,x,2(-x),x$, and for the $H_2N(COC_{\gamma/\beta})C_{\beta/\alpha}$ experiment: $\varphi_5 = 16(x),16(-x)$, and $\varphi_r = 2(x,-x),4(-x,x),2(x,-x),2(-x,x),4(x,-x),2(-x,x)$. Additional rf acquisition parameters were: sw(^{13}C) = 3.02 kHz, sw(^{15}N) = 1.22 kHz, sw(^1H) = 11.0 kHz, RD = 1.2 s, $t_1^{max} = 6.79$ ms, $t_2^{max} = 22.21$ ms, $t_3 = 70.0$ ms, $\tau_1 = 2.65$ ms, $\tau_2 = 5.56$ ms, $\tau_3 = 1.33$ ms, $\delta_1 = 11.5$ ms, $\delta_2 = 6.75$ ms, $\delta_3 = 0.0$ ms, $\delta_4 = 4.55$ ms, $\zeta = 1.2$ ms, $\gamma B_2(^{15}N_{decouple}) = 1.27$ kHz with WALTZ-16, and $\gamma B_4(^2H_{decouple}) = 1.01$ kHz with WALTZ-16. Gradient parameters were: $G_1 = -8$ G/cm, $t_{G1} = 0.4$ ms, $G_2 = -18$ G/cm, $t_{G2} = 1$ ms, $\Delta_2 = 2$ ms, $G_3 = -16$ G/cm, $t_{G3} = 0.4$ ms, $G_4 = -14$ G/cm, $t_{G4} = 0.8$ ms, $\Delta_4 = 1.6$ ms, $G_5 = -15$ G/cm, $t_{G5} = 0.8$ ms, $G_6 = -12$ G/cm, $t_{G6} = 2.5$ ms, $\Delta_6 = 5$ ms, $G_7 = -6$ G/cm, $t_{G7} = 1$ ms, $G_{7'} = -9$ G/cm, $t_{G7'} = 1$ ms, $G_8 = -15$ G/cm, $t_{G8} = 0.8$ ms, $\Delta_8 = 1.5$ ms, $G_9 = -22.5$ G/cm, $t_{G9} = 0.8$ ms, $G_{10} = -11$ G/cm, $t_{G10} = 0.7$ ms, $\Delta_{10} = 1.5$ ms, $G_{11} = -32.0$ G/cm, $t_{G11} = 5.0$ ms, $G_{12} = 30.2$ G/cm, $t_{G12} = 0.3$ ms, $G_{13} = -30.2$ G/cm, $t_{G13} = 0.4$ ms, $G_{14} = -32.03$ G/cm, and $t_{G14} = 0.5$ ms. Sixteen transients were collected per FID in the $H_2N(CO)C_{\gamma/\beta}$ experiment for a total acquisition time of 14.5 h. In the $H_2N(COC_{\gamma/\beta})C_{\beta/\alpha}$ experiment, 32 transients were collected per FID for a total acquisition time of 29 h. (C) The 3D $HN_\varepsilon C_\delta C_\gamma$ for assigning the side-chain $^1H_\varepsilon$/$^{15}N_\varepsilon$ amino resonances of arginine. The ^{13}C and ^{15}N carriers were set to 34 and 72 ppm, respectively.

C

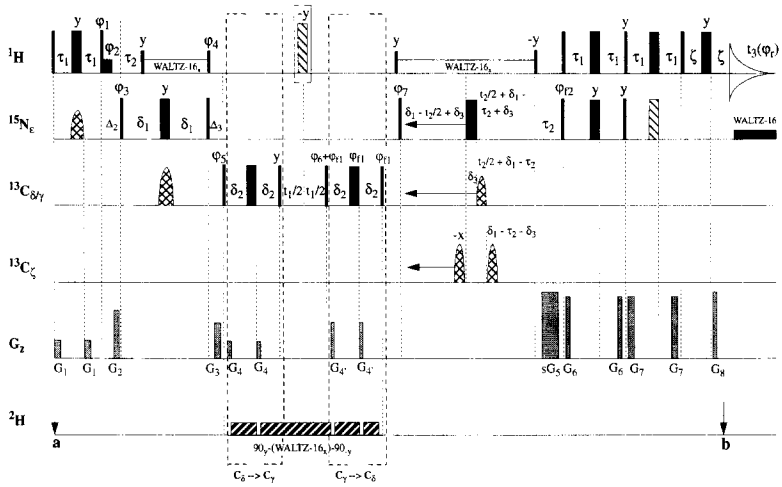

D

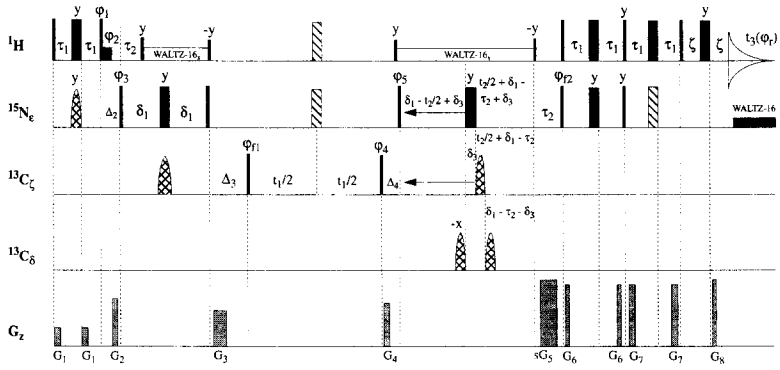

All C_ζ-selective pulses were frequency-shifted ~20 kHz to have a center excitation frequency at 167 ppm. C_ζ-selective and $C_{\delta/\gamma}$-selective G3-shaped inversion pulses had durations of 552 μs and 1.02 ms, respectively. The N_ε-selective G3-shaped inversion pulse had a duration of 1.73 ms. The water-selective 90° ^{1}H flipback pulse, labeled with phase φ_2, had a duration of 2.045 ms for $\varphi_1 = y$ and of 2.075 ms for $\varphi_1 = -y$. The t_1 evolution time was delayed by a half-dwell time in both experiments. Two separate 2D $H(N_\varepsilon)C_\delta$ and 2D $H(N_\varepsilon C_\delta)C_\gamma$ data sets were acquired. Common phase-cycle elements were: $\varphi_6 = 2(-y),2(y)$, and $\varphi_7 = y,-y$. $H(N_\varepsilon)C_\delta$ specific phase-cycle elements were: $\varphi_1 = 8(y),8(-y)$; $\varphi_2 = 8(193°),8(155°)$; $\varphi_3 = 4(x),4(-x)$; $\varphi_4 = -y$; $\varphi_5 = y$; and $\varphi_r = x,2(-x),x,-x,2(x),2(-x),2(x),-x,x,2(-x),x$. $H(N_\varepsilon C_\delta)C_\gamma$ specific phase-cycle elements were: $\varphi_1 = 16(y),16(-y)$; $\varphi_2 = 16(193°)$, $16(155°)$; $\varphi_3 = 8(x),8(-x)$; $\varphi_5 = 4(x),4(-x)$; and $\varphi_r = 2(x,-x),4(-x,x),2(x,-x),2(-x,x),4(x,-x),2(-x,x)$. For the spectra presented in Fig. 4, the ^{1}H inversion pulse in square brackets was omitted during t_1. If this ^{1}H inversion pulse is employed, $\varphi_4 = y$. Additional rf acquisition parameters were: sw(^{13}C) = 4.51 kHz, sw(^{1}H) = 11.0 kHz, RD = 3.0 s, $t_1^{max} = 9.19$ ms, $t_2^{max} = 0.0$ ms, $t_3 = 70.0$ ms, $\tau_1 = 2.65$ ms, $\tau_2 = 5.56$ ms, $\delta_1 = 15$ ms, $\delta_2 = 6.75$ ms, $\delta_3 = 0.0$ ms, $\zeta = 1.2$ ms, $\gamma B_1(^1H_{decouple}) = 3.91$ kHz, $\gamma B_2(^{15}N_{decouple}) = 1.12$ kHz, and $\gamma B_4(^2H_{decouple}) = 965$ Hz (all with WALTZ-16). Gradient parameters were: $G_1 = 8$ G/cm, $t_{G1} = 0.4$ ms, $G_2 = 18$ G/cm, $t_{G2} = 1$ ms, $\Delta_2 = 2$ ms, $G_3 = 14$ G/cm, $t_{G3} = 0.8$ ms, $\Delta_3 = 1.6$ ms, $G_4 = 6$ G/cm, $t_{G4} = 1$ ms, $G_{4'} = 12$ G/cm, $t_{G4'} = 1$ ms, $G_5 = 32$ G/cm, $t_{G5} = 5$ ms, $G_6 = -30.2$ G/cm, $t_{G6} = 0.3$ ms, $G_7 = 30.2$ G/cm, $t_{G7} = 0.4$ ms, $G_8 = 32.05$ G/cm, and $t_{G8} = 0.5$ ms. 256 transients were collected per FID for a total acquisition time of 19 h per experiment. (D) The refocused 3D $HN_\varepsilon C_\zeta$ for assigning the side-chain guanidino $^{13}C_\zeta$ resonances of arginine residues. The ^{13}C and ^{15}N carriers were set to 176 and 72 ppm, respectively. All C_δ-selective pulses were frequency-shifted ~−21 kHz to have a center excitation frequency at 36 ppm. C_ζ-selective and C_δ-selective G3-shaped inversion pulses had durations of 719 μs and 552 μs, respectively. The N_ε-selective G3-shaped inversion pulse had a duration of 1.73 ms. The water-selective 90° ^{1}H flipback pulse, labeled with phase φ_2, had a duration of 2.045 ms for $\varphi_1 = y$ and 2.075 ms for $\varphi_1 = -y$. The data were acquired as a 2D $H(N_\varepsilon)C_\zeta$ spectrum to achieve higher resolution in the $^{13}C_\zeta$ dimension. The t_1 evolution time was delayed by a half-dwell time. Phase-cycle elements were: $\varphi_1 = 8(y),8(-y)$; $\varphi_2 = 8(13.5°)$, $8(334°)$; $\varphi_3 = 4(x),4(-x)$; $\varphi_4 = 2(-y),2(y)$; $\varphi_5 = x,-x$; and $\varphi_r = x,2(-x),x,-x,2(x),2(-x),2(x),-x,x,2(-x),x$. Additional rf acquisition parameters were: sw(^{13}C) = 9 kHz, sw(^{1}H) = 11.0 kHz, RD = 1.2 s, $t_1^{max} = 21.28$ ms, $t_2^{max} = 0.0$ ms, $t_3 = 70.0$ ms, $\tau_1 = 2.65$ ms, $\tau_2 = 5.56$ ms, $\delta_1 = 12.5$ ms, $\delta_3 = 0.0$ ms, $\zeta = 1.2$ ms, $\gamma B_1(^1H_{decouple}) = 3.91$ kHz and $\gamma B_2(^{15}N_{decouple}) = 1.12$ kHz, both with WALTZ-16. Gradient parameters were: $G_1 = 8$ G/cm, $t_{G1} = 0.4$ ms, $G_2 = 18$ G/cm, $t_{G2} = 1$ ms, $\Delta_2 = 2$ ms, $G_3 = 14$ G/cm, $t_{G3} = 0.8$ ms, $\Delta_3 = 1.6$ ms, $G_4 = 12$ G/cm, $t_{G4} = 0.8$ ms, $\Delta_4 = 1.5$ ms, $G_5 = 32$ G/cm, $t_{G5} = 5$ ms, $G_6 = -30.2$ G/cm, $t_{G6} = 0.3$ ms, $G_7 = 30.2$ G/cm, $t_{G7} = 0.4$ ms, $G_8 = 32.05$ G/cm, and $t_{G8} = 0.5$ ms. Sixty-four transients were collected per FID for a total acquisition time of 15 h. (E) The nonrefocused 3D $HN_{\varepsilon,\eta}C_\zeta$ for linking the side-chain guanidino $^1H_\eta$ resonances to the C_ζ carbon in arginine residues. This pulse sequence was optimized for NH_2 groups. The ^{13}C and ^{15}N carriers were set to 162 and 62 ppm, respectively. No C_δ-selective pulses were applied in order to attenuate the $^1H_\varepsilon/^{13}C_\zeta$ correlation peaks. C_ζ-selective G3-shaped inversion pulses had a duration of 719 μs. The arginine N_ε-selective G3-shaped inversion pulse had a duration of 1.73 ms. The water-selective 90° ^{1}H flipback pulse, labeled with phase φ_2, had a duration of 2.065 ms for $\varphi_1 = y$ and of 2.085 ms for $\varphi_1 = -y$. The data were acquired as a 2D $H(N_{\varepsilon,\eta})C_\zeta$ spectrum in order to achieve higher resolution in the $^{13}C_\zeta$ dimension. Phase-cycle elements were: $\varphi_1 = 8(y),8(-y)$; $\varphi_2 = 8(13°),8(335°)$; $\varphi_3 = 4(x),4(-x)$; $\varphi_4 = 2(-y),2(y)$; $\varphi_5 = x,-x$; and $\varphi_r = x,2(-x),x,-x,2(x),2(-x),2(x),-x,x,2(-x),x$. Additional rf acquisition parameters were: sw(^{13}C) = 2 kHz, sw(^{1}H) = 11.0 kHz, RD = 1.2 s, $t_1^{max} = 74$ ms, $t_2^{max} = 0.0$ ms, $t_3 = 70.0$ ms, $\tau_1 = 2.65$ ms, $\tau_3 = 1.33$ ms, $\delta_1 = 12.5$ ms, $\delta_3 = 0.0$ ms, $\zeta = 1.2$ ms, and $\gamma B_2(^{15}N_{decouple}) = 1.12$ kHz with WALTZ-16. Gradient parameters were: $G_1 = 8$ G/cm, $t_{G1} = 0.4$ ms, $G_2 = 18$ G/cm, $t_{G2} = 1$ ms, $\Delta_2 = 2$ ms, $G_3 = 14$ G/cm, $t_{G3} = 0.8$ ms, $\Delta_3 = 1.6$ ms, $G_4 = 12$ G/cm, $t_{G4} = 0.8$ ms, $\Delta_4 = 1.5$ ms, $G_5 = 32$ G/cm, $t_{G5} = 2.5$ ms, $G_6 = -30.2$ G/cm, $t_{G6} = 0.3$ ms, $G_7 = 30.2$ G/cm, $t_{G7} = 0.4$ ms, $G_8 = 31.71$ G/cm, and $t_{G8} = 0.25$ ms. 128 transients were collected per FID for a total acquisition time of 15 h.

E

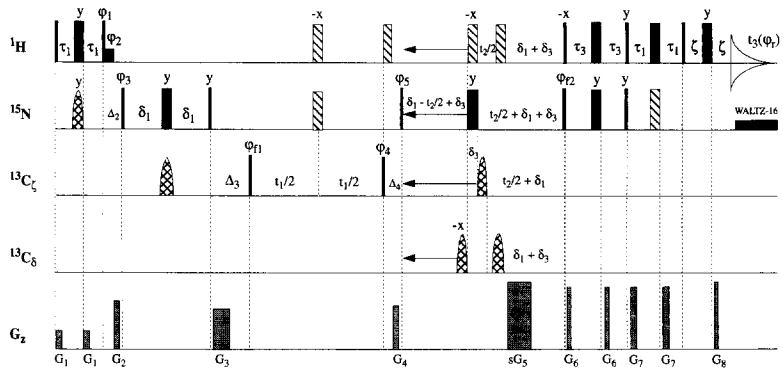

Fig. 1. (continued).

1995b). In this regard, side-chain hydrogen bonds have been shown to play an important role in the formation and stabilization of protein secondary structure (Borders et al., 1994; Bordo and Argos, 1994). Furthermore, it is empirically evident that NOEs involving side-chain aliphatic protons play a critical role in determining the structure of a protein. For these reasons, the assignment of NOE peaks involving side-chain H_N protons in a perdeuterated protein may be especially significant (Venters et al., 1995b). Six residue types contain side-chain H_N protons in a perdeuterated protein: asparagine, glutamine, arginine, lysine, tryptophan, and histidine. In this study, we focus on the assignment of such protons only from those residues with aliphatic side chains.

The traditional approach for assigning side-chain H_N protons is based on NOEs to intraresidue aliphatic protons, which have been previously assigned with either the HCCH-TOCSY (Bax et al., 1990; Kay et al., 1993) or the HC(CC)(CO)NH experiment (Montelione et al., 1992; Clowes et al., 1993; Grzesiek et al., 1993a; Logan et al., 1993). It has been noted that for small protonated proteins, the HC(CC)(CO)NH (Montelione et al., 1992), HC(CC)NH (Lyons and Montelione, 1993; Lyons et al., 1993), and HNCACB (Wittekind and Mueller, 1993) experiments can be parameterized so as to yield correlations between the side-chain NH_2 and aliphatic groups of asparagine and glutamine residues. Similarly, the HNHA-gly experiment has also yielded Arg $^1H_\varepsilon/^{13}C_\delta$ correlations (Wittekind et al., 1993). A strategy has also been proposed to obtain Arg $^1H_\varepsilon/^{13}C_\zeta$, $^1H_\varepsilon/^{15}N_\varepsilon$, and $^1H_\varepsilon/^{15}N_\eta$ correlations using both ^{15}N- and ^{13}CO-filtered 2D versions of the HNCO experiment, denoted as H(N)CZ and HN(CZ), respectively, and the 2D H(NCZ)N experiment (Vis et al., 1994). Finally, a set of optimized experiments, sufficient to completely assign the Arg ($^1H_\varepsilon$, $^{15}N_\varepsilon$, $^{13}C_\zeta$, $^{15}N_\eta$, $^1H_\eta$) resonances in protonated proteins, has been recently described (Yamazaki et al., 1995). Although all of these approaches have been shown to work on small protonated proteins, their extension to large, perdeuterated proteins for the purpose of side-chain $^1H_N/^{15}N$ resonance assignment has not been demonstrated and, furthermore, may encounter difficulty. Whereas the arginine $^1H_\delta$ resonances generally exhibit reasonable chemical-shift dispersion, the $^{13}C_\delta$ resonances are often overlapped. $^1H_\varepsilon/^{13}C_\delta$ correlations alone, obtained either with the HNHA-gly or truncated Arg-$H_\varepsilon(N_\varepsilon C_\delta)H_\delta$ (Yamazaki et al., 1995) experiment, may yield ambiguous assignments for some Arg $^1H_\varepsilon/^{15}N_\varepsilon$ resonances. The experiments for the identification of arginine guanidino spin systems (Vis et al., 1994; Yamazaki et al., 1995) appear amenable to large, perdeuterated proteins. In the absence of additional information, however, these experiments cannot be used to assign a guanidino spin system to a particular arginine residue, but rather only to identify the heteronuclear resonances involved in each such spin system.

To circumvent these potential problems, we have developed several gradient-enhanced and sensitivity-enhanced pulse sequences, containing water-flipback pulses (Grzesiek and Bax, 1993; Kay et al., 1994), to provide side-chain $^1H_N/^{15}N$ resonance assignments in large, perdeuterated proteins: NH_2-filtered 2D ^1H-^{15}N HSQC (H_2N-HSQC), 3D $H_2N(CO)C_{\gamma/\beta}$ and 3D $H_2N(COC_{\gamma/\beta})C_{\beta/\alpha}$ for glutamine and asparagine side-chain amide groups; and 2D refocused $H(N_{\varepsilon/\zeta})C_{\delta/\varepsilon}$ and $H(N_{\varepsilon/\zeta}C_{\delta/\varepsilon})C_{\gamma/\delta}$ for arginine side-chain amino groups as well as nonrefocused versions for lysine side-chain amino groups. For identifying and assigning the arginine guanidino resonances, we have enhanced the previously described 2D refocused $H(N_\varepsilon)C_\zeta$ and nonrefocused $H(N_{\varepsilon,\eta})C_\zeta$ experiments (Vis et al., 1994) by incorporating water-flipback techniques (Grzesiek and Bax, 1993; Yamazaki et al., 1995). The latter pulse sequence has also been optimized for NH_2 groups (Schleucher et al., 1994). All of these pulse sequences have been applied to perdeuterated ^{13}C-/^{15}N-labeled human carbonic anhydrase II (^2H-HCA II) (Venters et al., 1995a), a 29-kDa monomeric protein. Because more than 95% of all side-chain ^{13}C resonances in ^2H-HCA II have already been assigned with the C(CC)(CO)NH experiment (Farmer II and Venters, 1995), the assignment of the side-chain $^1H_N/^{15}N$ amide resonances of glutamine and asparagine and the amino resonances of arginine has been straightforward. Subsequently, we have utilized the argi-

nine C_ζ resonance to link assigned $^1H_\varepsilon/^{15}N_\varepsilon$ resonances to unassigned $^1H_\eta/^{15}N_\eta$ resonances in these residues. A similar approach has already been described for using the N9 resonance to link the ribose $^1H1'/^{13}C1'$ resonances to the base $^1H8/^{13}C8$ resonances in purine nucleotides of $^{13}C/^{15}N$ isotopically labeled RNA (Farmer II et al., 1994). The overall importance of assigning these side-chain H_N protons in perdeuterated proteins has been demonstrated by recent studies in which the calculation of protein global folds has been simulated using only ^1H_N-^1H_N NOE restraints (Venters et al., 1995b). In these studies, the inclusion of NOE restraints to side-chain H_N protons significantly improved the quality of the global fold that could be determined for a perdeuterated protein.

Results

The preparation of HCA II, up to 96% ^2H-labeled on aliphatic sites, has been previously described (Venters et al., 1995a). All spectral data were collected at 30.0 °C on a 1.6 mM ^2H-/^{13}C-/^{15}N-labeled HCA II sample in 100 mM phosphate buffer at pH 6.8. A four-channel Varian UnityPlus 600 MHz spectrometer, equipped with ^2H broadband decoupling capability and a 5 mm $^1H/^{13}C/^{15}N$ triple-resonance probe having an actively shielded z-gradient, was used for data acquisition. The data were subsequently processed either on a Sun Sparc 10-41 using VNMR 5.1 software (Varian Associates, Palo Alto, CA) or on an SGI Indigo2 Extreme using an extensively modified version of FELIX 1.0 (Hare Research, Inc, Bothell, WA). Because a relatively high pH (6.8) is necessary for HCA II to remain stable in solution, the use of water-flipback techniques (Grzesiek and Bax, 1993; Kay et al., 1994) was deemed crucial to the assignment of the side-chain aliphatic $^1H_N/^{15}N$ resonances.

Glutamine/asparagine residues

The NH_2-HSQC pulse sequence depicted in Fig. 1A has been used to identify the side-chain $^1H_N/^{15}N$ resonances of glutamine and asparagine residues and the $H_2N(CO)C_{\gamma/\beta}$ and $H_2N(COC_{\gamma/\beta})C_{\beta/\alpha}$ pulse sequences depicted in Fig. 1B have subsequently been utilized to assign these side chains. The basic framework for the above sequences is derived from gradient-enhanced and sensitivity-enhanced versions of the NH-HSQC (Kay et al., 1992), HN(CO)CA and HN(COCA)CB (Kay et al., 1990,1994; Yamazaki et al., 1994a) pulse sequences, respectively, which have been used to make sequential backbone resonance assignments. The sequences presented here also minimize the saturation of water magnetization by using water-flipback techniques (Grzesiek and Bax, 1993; Yamazaki et al., 1995) and incorporate broadband ^2H decoupling when necessary for deuterated proteins. As presented in Figs. 1A and B, we have re-designed the original sequences so that they are both optimum and selective for side-chain NH_2 groups in perdeuterated proteins.

NH_2 filtering is a key component of the new sequences. In short, the filtering scheme relies on the fact that NH_2 $^{15}N_xH_z$ antiphase magnetization remains antiphase to ^1H_N

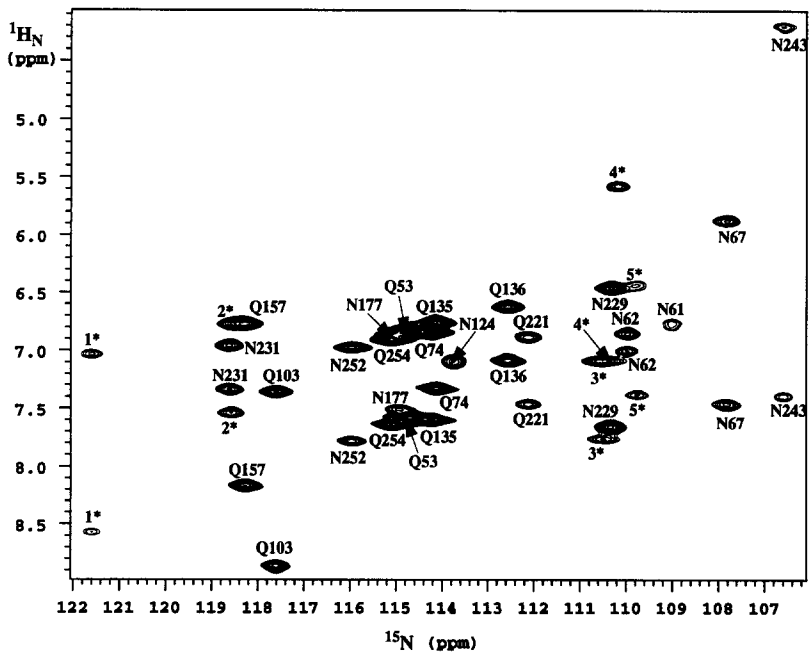

Fig. 2. A 2D ^1H-^{15}N NH_2-HSQC spectrum acquired with the pulse sequence in Fig. 1A. Nine of 10 asparagine and 8 of 11 glutamine side-chain $^1H_N/^{15}N$ amide-resonance pairs have been assigned; only those of Asn^{11}, Gln^{28}, Gln^{92}, and Gln^{128} remain unassigned. The chemical shifts for the Asn ($H_{\delta 21}$, $H_{\delta 22}$, $N_{\delta 2}$) and Gln ($H_{\varepsilon 21}$, $H_{\varepsilon 22}$, $N_{\varepsilon 2}$) resonances are summarized in Table 1. By our convention, the chemical shifts of $H_{\delta 21}$ and $H_{\varepsilon 21}$ are always upfield from those of $H_{\delta 22}$ and $H_{\varepsilon 22}$, respectively. Five pairs of resonances in this spectrum, labeled 1* through 5*, are currently unassigned.

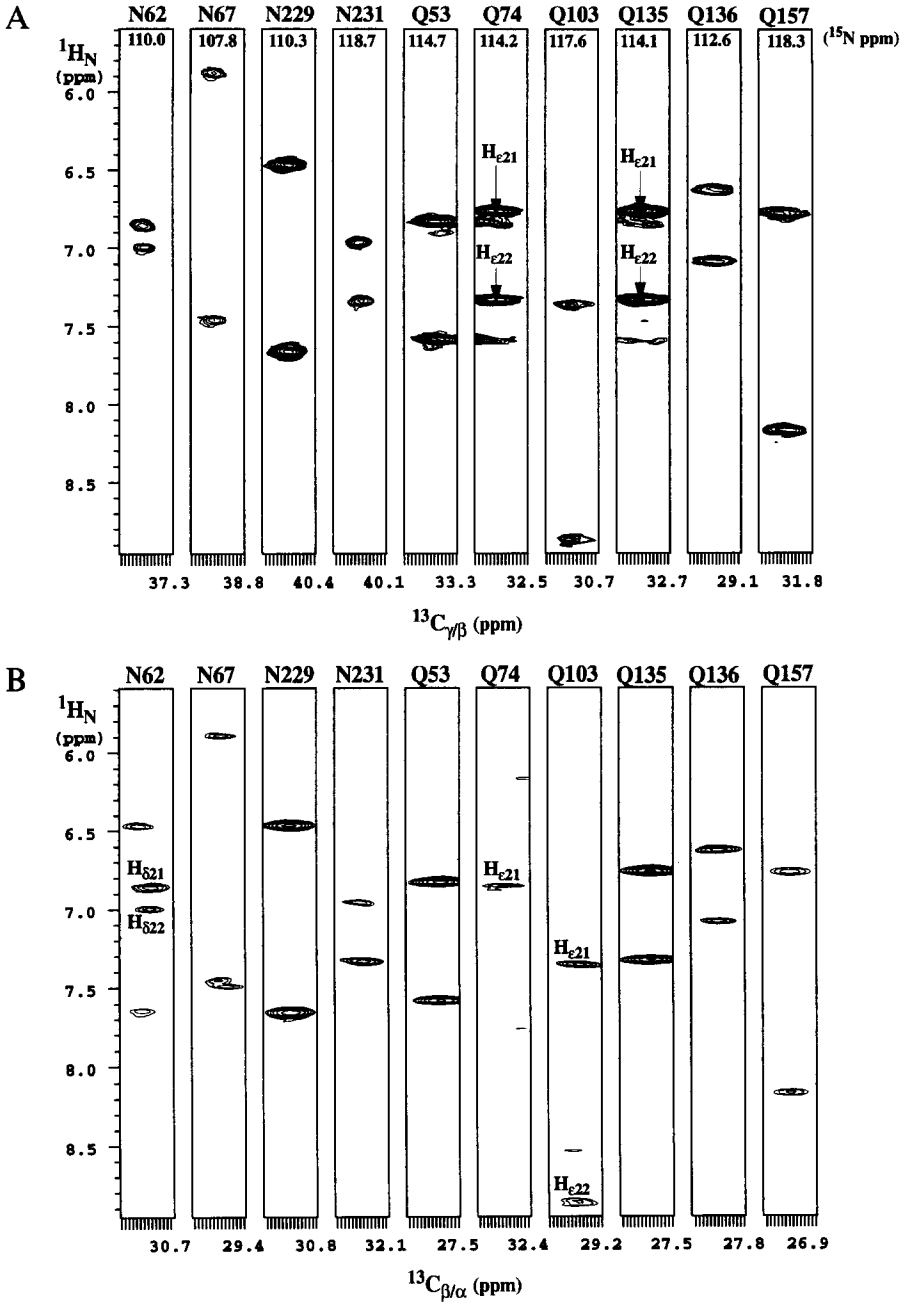

Fig. 3. (A) $^{13}C_{\gamma/\beta}/^{1}H_N$ strip plots from the 3D $H_2N(CO)C_{\gamma/\beta}$ spectrum (Fig. 1B). These data yield the ^{13}C chemical shift of the asparagine C_β and glutamine C_γ resonances. All correlations have been phased for positive intensity. (B) $^{13}C_{\beta/\alpha}/^{1}H_N$ strip plots from the 3D $H_2N(COC_{\gamma/\beta})C_{\beta/\alpha}$ spectrum. These data yield the ^{13}C chemical shifts of the asparagine C_α and glutamine C_β resonances. In this spectrum, the glutamine and asparagine correlations have negative and positive intensities, respectively, due to aliasing of the asparagine C_α resonances under a half-dwell-time delay in t_1. The assignment of the $^{1}H_N/^{15}N$ resonances has been made by correlating the $^{13}C_\gamma/C_\beta$ or $^{13}C_\beta/C_\alpha$ chemical shifts obtained in these spectra with those of glutamine or asparagine residues, respectively, which had been previously assigned from HNCACB (Venters et al., 1995a) and C(CC)(CO)NH (Farmer II and Venters, 1995) spectra.

even after a delay of $1/(2J_{NH})$ (τ_2 in Fig. 1). In contrast, NH $^{15}N_xH_z$ antiphase magnetization refocuses to ^{15}N in-phase magnetization during this delay. Consequently, only the NH_2 $^{15}N_xH_z$ antiphase magnetization survives the subsequent ^{1}H single-quantum filter. In addition, sensitivity for NH_2 groups has been maximized in the following two ways. Firstly, the initial echo period in the sensitivity-enhanced (SE) subsequence (Kay et al., 1992), labeled as τ_3 in Figs. 1A and B, is set to a value of $1/(4J_{NH})$, the optimum value for NH_2 groups (Schleucher et al., 1994). Secondly, the $^{15}N_xH_z$ antiphase magnetization is not refocused with respect to $^{1}H_N$ during the first pair of δ_1 delays (Fig. 1B) and therefore does not need to be defocused again later on in the pulse sequence. For NH groups, one normally refocuses the $^{15}N_xH_z$ antiphase magnetization during the first δ_1 delay and then defocuses

the resulting in-phase magnetization with respect to ^1H_N during the last part of the ^{15}N constant-time evolution period. When this approach is applied to NH_2 groups, a twofold loss in relative sensitivity is incurred.

Figure 2 presents the ^1H-^{15}N NH_2-HSQC spectrum on ^2H-HCA II, acquired with the pulse sequence of Fig. 1A. This spectrum allows the identification of ^1H_N / ^{15}N resonances with high sensitivity from all NH_2 groups, excluding those from arginine residues. The actual assignment of the resonances shown in Fig. 2, however, is achieved with the pulse sequence in Fig. 1B. The $H_2N(CO)C_{\gamma/\beta}$ experiment, which is NH_2-filtered, correlates both Gln ($^1H_{\varepsilon 21,22}$, $^{15}N_{\varepsilon 2}$, $^{13}C_\gamma$) resonances and Asn ($^1H_{\delta 21,22}$, $^{15}N_{\delta 2}$, $^{13}C_\beta$) resonances; the corresponding $H_2N(COC_{\gamma/\beta})C_{\beta/\alpha}$ experiment correlates both Gln ($^1H_{\varepsilon 21,22}$, $^{15}N_{\varepsilon 2}$, $^{13}C_\beta$) resonances and Asn ($^1H_{\delta 21,22}$, $^{15}N_{\delta 2}$, $^{13}C_\alpha$) resonances. The preservation of water magnetization by this pulse sequence has been assessed by using a 20 s relaxation delay and adding the following pulse elements immediately prior to ^1H_N detection: G_z (32 G/cm for 3 ms), 3 ms delay, 1 μs pulse with $\gamma B(^1H) \sim 4$ kHz, acquire data (L. Mueller, personal communication). The integrated intensity of the remaining water magnetization measured in this way is then compared to the integrated intensity of equilibrium water magnetization obtained with the following simple sequence: 20 s relaxation delay, 1 μs pulse with $\gamma B(^1H) \sim 4$ kHz, acquire data. With this method, the $H_2N(CO)C_{\gamma/\beta}$-$C_{\beta/\alpha}$ pulse sequence has been shown to preserve 58–72% of the total water magnetization.

2D ^{13}C / ^1H_N strip plots from the 3D $H_2N(CO)C_{\gamma/\beta}$ and $H_2N(COC_{\gamma/\beta})C_{\beta/\alpha}$ experiments are presented in Figs. 3A and B, respectively. Some of the correlation peaks in Fig. 3 are quite intense; others are rather weak. It is tempting to speculate that the weak correlations arise in glutamine/asparagine residues, the side chains of which are less mobile and may therefore be more structured. By matching the Gln $^{13}C_\gamma/C_\beta$ and Asn $^{13}C_\beta/C_\alpha$ chemical shifts to those previously obtained with the HNCACB (Yamazaki et al., 1994a; Venters et al., 1995a) and C(CC)(CO)NH (Farmer II and Venters, 1995) experiments, the assignment of these side-chain ^1H_N / ^{15}N resonances can be completed. We have done this for ^2H-HCA II; the results are presented in Table 1. Only the resonances for Asn^{11}, Gln^{28}, Gln^{92}, and Gln^{248} remain unassigned. For seven asparagine residues, there is sufficient chemical-shift dispersion in the C_β resonances alone to assign the side-chain ^1H_N / ^{15}N resonances. For the remaining two observable asparagine residues, Asn^{61} and Asn^{62}, the increased chemical-shift difference between their $^{13}C_\alpha$ resonances (0.25 ppm) relative to their $^{13}C_\beta$ resonances (0.08 ppm) has been sufficient to permit the correct ^1H_N / ^{15}N assignments. The assignment of ^1H_N / ^{15}N resonances in Figs. 2 and 3 to particular glutamine side-chain amide groups has been more difficult. Firstly, three glutamine residues, Gln^{74}, Gln^{136}, and Gln^{248}, are missing C_γ assignments from the C(CC)(CO)NH experiment. This is understandable for Gln^{136} and Gln^{248}, since both residues are in the i–1 position to a proline. Secondly, the $^{13}C_\gamma$ chemical shifts for Gln^{53} and Gln^{254} are indistinguishable. For these two reasons, the $^1H_{\varepsilon 21,22}/^{15}N_{\varepsilon 2}/^{13}C_\beta$ correlations in glutamine residues have proven to be of greater utility than the corresponding correlations in asparagine residues. In total, the side-chain ^1H_N / ^{15}N resonances for eight glutamine residues have been assigned. The other three glutamine residues yield no observable correlations in the $H_2N(CO)C_{\gamma/\beta}$ spectrum (Fig. 3A) and no resolved correlations in the $H_2N(COC_{\gamma/\beta})C_{\beta/\alpha}$ spectrum (Fig. 3B). Finally, these experiments have also provided the $^{13}C_\gamma$ chemical shifts for Gln^{74} and Gln^{136}.

Arginine residues

Arginine side chains in a perdeuterated protein contain a wealth of potentially observable and therefore assignable H_N resonances. Two types of side-chain H_N protons exist for arginine: one H_ε secondary amino proton and four H_η guanidino protons. The $^{15}N_\varepsilon$ resonance typically occurs between 80–88 ppm (Yamazaki et al., 1995). The $^{15}N_\eta$ resonance lies slightly more upfield, typically occurring between 69–74 ppm (Yamazaki et al., 1995). We have focused initially on the H_ε protons for three reasons. Firstly, these protons appear readily assignable based on correlations to side-chain $^{13}C_{\delta/\gamma}$ resonances. Secondly,

TABLE 1
^1H AND ^{15}N CHEMICAL SHIFTS FOR ASPARAGINE AND GLUTAMINE SIDE-CHAIN AMIDE GROUPS

Residue	$N_{\delta 2}$	$H_{\delta 21}$	$H_{\delta 22}$	Residue	$N_{\varepsilon 2}$	$H_{\varepsilon 21}$	$H_{\varepsilon 22}$
Asn^{61}	109.0	6.758		Gln^{53}	114.7	6.825	7.577
Asn^{62}	110.0	6.853	6.993	Gln^{74}	114.2	6.847	7.596
Asn^{67}	107.8	5.878	7.463	Gln^{103}	117.6	7.357	8.861
Asn^{124}	113.7	7.049	7.097	Gln^{135}	114.1	6.758	7.325
Asn^{177}	115.0	6.858	7.502	Gln^{136}	112.6	6.623	7.081
Asn^{229}	110.3	6.463	7.656	Gln^{157}	118.3	6.772	8.166
Asn^{231}	118.7	6.958	7.331	Gln^{221}	112.1	6.884	7.464
Asn^{243}	106.6	4.191	7.397	Gln^{254}	115.1	6.905	7.638
Asn^{252}	116.0	6.973	7.785				

Side-chain amide groups for Asn^{11}, Gln^{28}, Gln^{92}, and Gln^{248} remain unassigned.

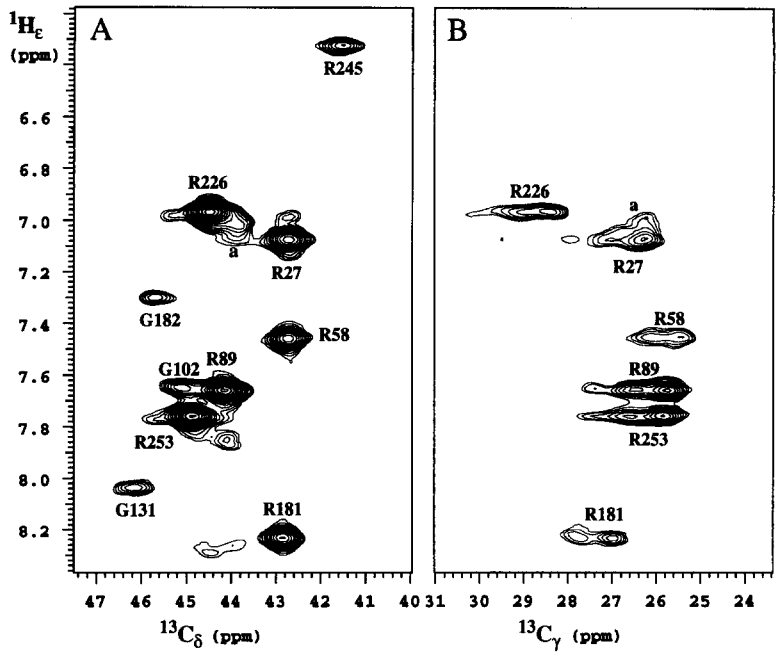

Fig. 4. (A) A 2D $^1H_\varepsilon/^{13}C_\delta$ correlation spectrum acquired with the $H(N_\varepsilon)C_\delta$ pulse sequence in Fig. 1C. Selectivity is implemented on ^{15}N during only the initial $^1H_N \rightarrow {}^{15}N$ INEPT transfer and on ^{13}C during both the forward and reverse $^{15}N_\varepsilon \rightarrow {}^{13}C_\delta$ INEPT transfers. Backbone $^1H_N/{}^{13}C_\alpha$ correlations for three glycine residues with upfield shifted ^{15}N resonances (~100 ppm) are also present, but with decreased intensity. Four arginine $^1H_\varepsilon/{}^{13}C_\delta$ correlations are easily assigned based only on the $^{13}C_\delta$ chemical shift: Arg^{89}, Arg^{226}, Arg^{245}, and Arg^{253}. The $^{13}C_\delta$ resonances of Arg^{27}, Arg^{58}, and Arg^{181} are too overlapped for an unambiguous assignment to be made. Peak 'a' is discussed in the legend to Fig. 5C. (B) A 2D $^1H_\varepsilon/{}^{13}C_\gamma$ correlation spectrum acquired with the $H(N_\varepsilon C_\delta)C_\gamma$ pulse sequence (Fig. 1C). The $^1H_\varepsilon$ assignments for Arg^{27}, Arg^{58}, and Arg^{181} can now be made based on the $^{13}C_\gamma$ chemical shift of the respective $^1H_\varepsilon/{}^{13}C_\gamma$ correlation. The ^{13}C lineshape for the C_γ carbons presents an interesting multiplet-like structure. It is important to note that the ^1H-^{13}C scalar coupling has not been refocused during the ^{13}C t_1 evolution period. The details of the arginine C_γ lineshape are explained in Fig. 6.

these protons can be easily correlated with the C_ζ carbon through an HNCZ experiment (Vis et al., 1994), which is based on the HNCO experiment (Kay et al., 1990,1994). Finally, the H_ε protons are in general much less susceptible than the H_η protons to rapid exchange with the solvent water and are therefore more likely to yield observable ^1H_N-^1H_N NOEs.

Due to the absence of aliphatic side-chain protons in ^{2}H-HCA II, we have used a slightly different approach in assigning the arginine $^1H_\varepsilon/{}^{15}N_\varepsilon$ resonances than previous authors (Wittekind et al., 1993; Yamazaki et al., 1995). The particular pulse sequence for making the $^1H_\varepsilon$ assignments is presented in Fig. 1C. It is derived from the HNCACB experiment (Wittekind and Mueller, 1993; Yamazaki et al., 1994a; Venters et al., 1995a). The $^1H \rightarrow {}^{15}N$ forward INEPT transfer is selective for ^{15}N resonances in the range 56–88 ppm (≥95% inversion), with ≥95% rejection of all resonances with ^{15}N chemical shifts downfield of 106 ppm. This is achieved with a G3 ^{15}N inversion pulse of 1.73 ms duration, centered at 72.3 ppm. The refocused nature of the ^1H-^{15}N INEPT and reverse INEPT transfers greatly attenuates all NH_2 groups, such as side-chain glutamine/asparagine amide protons and arginine guanidino protons.

Figures 4A and B present the arginine $^1H_\varepsilon/{}^{13}C_\delta$ and $^1H_\varepsilon/{}^{13}C_\gamma$ correlations, respectively, obtained with the pulse sequence in Fig. 1B. The optional '$C_\delta \rightarrow C_\gamma$' forward and reverse transfer steps are utilized in this sequence to obtain the $^1H_\varepsilon/{}^{13}C_\gamma$ correlations. All seven arginine $^1H_\varepsilon/{}^{13}C_\delta$ correlations, but only six $^1H_\varepsilon/{}^{13}C_\gamma$ correlations, are observed. The $^1H_\varepsilon$ resonances for Arg^{89}, Arg^{226}, Arg^{245}, and Arg^{253} have been assigned directly from the $^1H_\varepsilon/{}^{13}C_\delta$ spectrum (Fig. 4A). The $^{13}C_\delta$ chemical shifts of Arg^{27}, Arg^{58}, and Arg^{181}, however, are too similar for an unambiguous assignment to be made based solely on these $^1H_\varepsilon/{}^{13}C_\delta$ correlation data. The $^1H_\varepsilon/{}^{13}C_\gamma$ correlation data in Fig. 4B resolve the ambiguity in the $^1H_\varepsilon$ assignment for these three arginine residues. Backbone $^1H_N/{}^{13}C_\alpha$ correlations for several glycine residues with upfield ^{15}N chemical shifts (~99–101 ppm) can also be observed in Fig. 4A. These correlations, however, are noticeably weaker than the arginine $^1H_\varepsilon/{}^{13}C_\delta$ correlations. In order to assign the seven arginine $^{15}N_\varepsilon$ resonances, a 2D $HN_\varepsilon(C_\zeta)$ spectrum has been acquired with the pulse sequence in Fig. 1D. Due both to the large chemical-shift dispersion for the arginine H_ε protons in ^{2}H-HCA II and to the sufficiently unique $^{15}N_\varepsilon$ chemical shifts of these residues in general, a 2D experiment was found to be sufficient in this regard.

Having assigned the arginine $^1H_\varepsilon/{}^{15}N_\varepsilon$ resonances, we are now left with first identifying and then assigning the guanidino $^1H_\eta/{}^{15}N_\eta$ resonances. Since many of these protons will exchange rapidly with solvent water protons, we

have acquired a gradient-enhanced ^{1}H-^{15}N HSQC spectrum (Kay et al., 1992) with water flipback (Grzesiek and Bax, 1993; Kay et al., 1994), in which the first echo period of the SE subsequence is set to $1/(4J_{NH})$ (Schleucher et al., 1994). Any arginine H_η proton that is not observable with this experiment is assumed to exchange rapidly with the solvent water protons and is therefore not expected to yield an observable NOE in any ^{15}N-separated NOESY. Only five potential $^{1}H_\eta/^{15}N_\eta$ correlations are visible in this HSQC spectrum (Fig. 5C) for the seven arginine residues. To assign these resonances, we have relied on the intrinsic chemical-shift dispersion within the arginine $^{13}C_\zeta$ resonances in ^{2}H-HCA II.

Figure 5A presents the $^{1}H_\varepsilon/^{13}C_\zeta$ correlation spectrum, obtained with the refocused 2D $H(N_\varepsilon)C_\zeta$ pulse sequence depicted in Fig. 1D. This pulse sequence has been shown to preserve 56% of the total water magnetization. As with the $^{1}H_\varepsilon/^{13}C_{\delta/\gamma}$ correlation experiments for arginine residues, the $^{1}H \rightarrow {}^{15}N$ forward INEPT transfer employs a selective G3 inversion pulse on ^{15}N, centered at 72.3 ppm and having a duration of 1.73 ms. In addition, the refocused nature of the ^{1}H-^{15}N forward and reverse INEPT transfers greatly attenuates all NH_2 groups. In this way, only arginine $^{1}H_\varepsilon/^{13}C_\zeta$ correlations are retained with any appreciable intensity. There are two reasons why the arginine C_ζ carbon is ideal in its role as a chemical-shift link between the side-chain $^{1}H_\varepsilon$ and $^{1}H_\eta$ resonances: (i) it has no appreciable homonuclear ^{13}C scalar coupling; and (ii) it exhibits relatively long T_2 values. Both of these reasons impact the achievable resolution within these carbon resonances. High resolution within the $^{13}C_\zeta$ resonances is also more easily obtained in 2D experiments. As a direct result of the above considerations, we have been able to easily distinguish the $^{13}C_\zeta$ resonance of Arg^{89} from that of Arg^{226} ($\Delta\sigma(^{13}C_\zeta) \sim 0.11$ ppm). In fact, all seven $^{13}C_\zeta$ resonances for ^{2}H-HCA II are sufficiently resolved in the 2D $^{1}H_\varepsilon/^{13}C_\zeta$ spectrum (Fig. 5A).

In a similar fashion, arginine $^{1}H_\eta/^{13}C_\zeta$ correlations have been obtained with the nonrefocused version of the $H(N_{\varepsilon,\eta})C_\zeta$ experiment depicted in Fig. 1E. The 2D $^{1}H_{\varepsilon,\eta}/^{13}C_\zeta$ spectrum is shown in Fig. 5B. An analysis of the correlations in both Figs. 5A and B yields the assignment of the H_η protons for three distinct arginine residues: Arg^{27}, Arg^{245}, and Arg^{253}. The associated $^{15}N_\eta$ chemical shifts are readily determined from a $^{15}N_{\varepsilon,\eta}$-selective ^{1}H-^{15}N HSQC experiment optimized for NH_2 groups (Fig. 5C). The

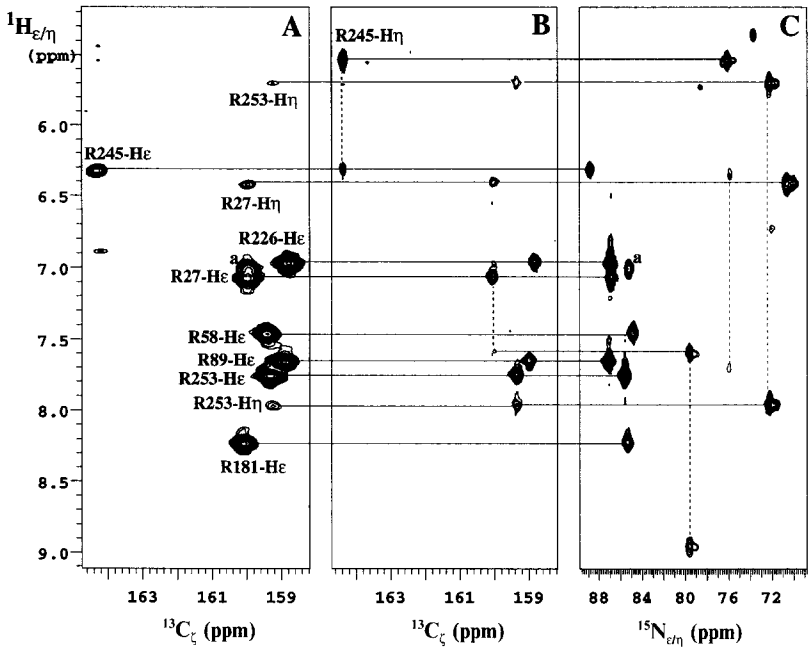

Fig. 5. (A) A 2D $^{1}H_\varepsilon/^{13}C_\zeta$ correlation spectrum acquired with the refocused $H(N_\varepsilon)C_\zeta$ pulse sequence in Fig. 1D. All seven arginine $^{1}H_\varepsilon/^{13}C_\zeta$ correlations are observed. Three $^{1}H_\eta/^{13}C_\zeta$ correlations are also present in the spectrum. Because of the large dispersion in $^{1}H_\varepsilon$ chemical shifts and the limited number of arginine residues in HCA II, the $^{13}C_\zeta$ resonances have been assigned using only this 2D spectrum. The level of chemical-shift resolution achievable within this set of $^{13}C_\zeta$ resonances is also demonstrated and suggests that the C_ζ carbon can serve as a chemical-shift link to the arginine $^{1}H_\eta/^{15}N_\eta$ resonances. (B) A 2D $^{1}H_{\varepsilon,\eta}/^{13}C_\zeta$ correlation spectrum acquired with the nonrefocused $H(N_{\varepsilon,\eta})C_\zeta$ pulse sequence, optimized for NH_2 groups (Fig. 1E). This spectrum has yielded a previously unobserved Arg^{245} $^{1}H_\eta/^{13}C_\zeta$ correlation and increased intensity for the other two Arg^{253} $^{1}H_\eta/^{13}C_\zeta$ correlations, compared to Fig. 5A. The assignment of the arginine $^{1}H_\eta$ resonances is made through correlations to previously assigned $^{13}C_\zeta$ resonances. (C) A 2D $^{1}H_{\varepsilon,\eta}/^{15}N_{\varepsilon,\eta}$ correlation spectrum acquired with the standard gradient-enhanced, sensitivity-enhanced ^{1}H-^{15}N HSQC pulse sequence (Kay et al., 1992), optimized for NH_2 groups (Schleucher et al., 1994). Two additional sets of unassigned correlation peaks are observed. The two peaks in each set are linked by a vertical, dashed line. The most intense set definitely represents two $^{1}H_\eta/^{15}N_\eta$ correlations, based on the observed upfield 'partner' peaks, and has been tentatively assigned to Arg^{27}. The peak labeled 'a' is thought to arise from a second species of Arg^{27}. Its correlation to a carbon with a $^{13}C_\zeta$ chemical shift (Fig. 5A), its ^{15}N chemical shift, and the absence of an upfield 'partner' peak indicate that peak 'a' represents an Arg $^{1}H_\varepsilon/^{13}C_\zeta$ correlation.

TABLE 2
^{1}H, ^{15}N AND ^{13}C CHEMICAL SHIFTS FOR ARGININE SIDE-CHAIN AMINO AND GUANIDINO GROUPS

Residue	H_ε	N_ε	C_ζ	$N_{\eta 1}$	$H_{\eta 1}$	$N_{\eta 2}$	$H_{\eta 2}$
Arg^{27}	7.115	86.9	160.1	70.7	6.451	79.7	7.634, 8.987
Arg^{58}	7.499	84.9	159.5				
Arg^{89}	7.696	87.1	159.0				
Arg^{181}	8.268	85.4	160.1				
Arg^{226}	7.007	87.0	158.9				
Arg^{245}	6.363	88.8	164.3	76.2	5.581		
Arg^{253}	7.794	85.6	159.5	72.3	5.742, 7.992		

Only Arg^{27}, Arg^{245}, and Arg^{253} yield observable $^{1}H_\eta/^{15}N_\eta$ guanidino resonances.

$^{15}N_{\varepsilon,\eta}$ selectivity is achieved in the same manner as for the 2D $H(N_\varepsilon)C_\zeta$ and $H(N_{\varepsilon,\eta})C_\zeta$ spectra in Figs. 5A and B. Table 2 summarizes the arginine side-chain ($^{1}H_\varepsilon$, $^{15}N_\varepsilon$, $^{13}C_\zeta$, $^{15}N_\eta$, $^{1}H_\eta$) resonance assignments for ^{2}H-HCA II. The crystal structure of HCA II indicates that the side chains of Arg^{27}, Arg^{245}, and Arg^{253} are directed back into the protein core (Liljas et al., 1972). The observation in Fig. 5 of at least one H_η proton on each of these three arginine residues is consistent with the X-ray results.

Several of the experiments proposed by Yamazaki et al. (1995) for assigning arginine guanidino groups utilize a ^{13}C-^{15}N heteroTOCSY spin-lock to transfer $^{13}C_\zeta$ magnetization to $^{15}N_\eta$ (and back) and therefore suffer less degradation in sensitivity due to moderate rotational exchange of the NH_2 η groups about the C_ζ-N_ε bond. The $N_\eta \rightarrow C_\zeta$ forward and reverse INEPT transfers used in Fig. 1E tend to select for those arginine side-chain guanidino groups for which the rotation about the C_ζ-N_ε bond is hindered structurally, due either to packing considerations or to specific hydrogen bonding interactions with one or both of the NH_2 η groups. The INEPT transfer can therefore be considered to select for those arginine side-chain guanidino groups that are more relevant to the determination of a stable tertiary structure.

There are several additional aspects of Fig. 5 that deserve comment. The peaks labeled 'a' in Figs. 5A and C are thought to belong to a subpopulation of Arg^{27}, whose side chain adopts a different conformation and/or makes alternative H-bonding interactions. That these correlations arise from NH and not from NH_2 or NH_3 groups is deduced from the absence of any 'partner' peak(s) due to the ^{2}H isotope effect on the ^{15}N chemical shift of NHD, NH_2D, or NHD_2 moieties. This proposed subpopulation of Arg^{27} exhibits $^{1}H_\varepsilon$ and $^{15}N_\varepsilon$ chemical shifts that are slightly more upfield than those of the main population. Arg^{27} also presents anomalies in its $^{13}C_\delta$ chemical shift. The main Arg^{27} C_δ peak in Fig. 4A has a ^{13}C chemical shift of 42.7 ppm. The peak labeled 'a' in Fig. 4A has a ^{13}C chemical shift of ~43.8 ppm and is thought to correspond to this subpopulation of Arg^{27}. A similar Arg^{27} C_γ peak ('a') exists in Fig. 4B, but does not differ significantly in its ^{13}C chemical shift from that of the main Arg^{27} C_γ peak.

Arginine and glutamine C_γ multiplet

The arginine side-chain $^{1}H_\varepsilon/^{13}C_\delta$ correlations in Fig. 4A appear as single peaks; the $^{1}H_\varepsilon/^{13}C_\gamma$ correlations in Fig. 4B, however, present an asymmetric multiplet-like pattern. This pattern complicates the assignment of the arginine $^{13}C_\gamma$ resonances based on the C(CC)(CO)NH-derived $^{13}C_\gamma$ chemical shifts. A closer examination has revealed that the average chemical shift for the two most intense peaks in the arginine $^{1}H_\varepsilon/^{13}C_\gamma$ multiplets in Fig. 4B matches the chemical shift obtained for the respective $^{13}C_\gamma$ resonances in the C(CC)(CO)NH experiment. The ^{13}C trace through the $^{1}H_\varepsilon/^{13}C_\gamma$ multiplet of Arg^{89} is presented in Fig. 6 and reveals an asymmetric distribution of peak intensities. To understand this multiplet-like pattern, it must first be recognized that for the arginine side-chain $H(NC_\delta)C_\gamma$ spectrum, the ^{1}H-^{13}C scalar coupling has not been refocused during the ^{13}C t_1 evolution period as it has been in the C(CC)(CO)NH experiment. Additionally, the

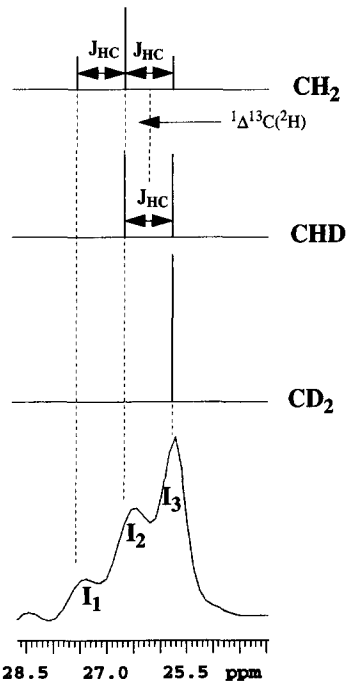

Fig. 6. The ^{13}C F_1 trace through the Arg^{89} $^{1}H_\varepsilon/^{13}C_\gamma$ correlation peak from Fig. 4B. The F_1 multiplet-like structure of this peak is analyzed in terms of a superposition of resonances from CH_2, CHD, and CD_2 groups.

one-bond ^2H isotope shift on the observed $^{13}C_\gamma$ chemical shift, $^1\Delta^{13}C_\gamma(^2H)$, is estimated to be ~ -0.4 ppm per deuteron, based on the value obtained for propane-2-d_1 (Wesener et al., 1985). $^1\Delta^{13}C_\gamma(^2H)$ is essentially equivalent in magnitude to $J_{CH}/2$ for a methylene group. Figure 6 depicts the analysis of this multiplet-like pattern in terms of a superposition of three types of arginine C_γ groups: CH_2, CHD, and CD_2. The most downfield peak, which is quite weak in intensity, arises from the $m=+1$ multiplet line of the CH_2 group. The center peak is a superposition of the $m=0$ multiplet line from the CH_2 group and the $m=+1/2$ line from the CHD group. Note that both multiplet lines of the CHD group are shifted upfield by $^1\Delta^{13}C_\gamma(^2H)$ (~ 60 Hz). Finally, the most upfield peak has contributions from all three groups: the $m=-1$ line from the CH_2 group, the $m=-1/2$ line from the CHD group, and the singlet line from the CD_2 group. The populations for the three arginine C_γ groups can be determined from the following equations:

$$P_{CH_2} = 4I_1 / I_{tot} \quad (1a)$$

$$P_{CHD} = 2(I_2 - 2I_1) / I_{tot} \quad (1b)$$

$$P_{CD_2} = (I_3 - I_2 + I_1) / I_{tot} \quad (1c)$$

where

$$I_{tot} = I_3 + I_2 + I_1 \quad (2)$$

and I_i represents the intensity of peak i in Fig. 6. We have analyzed the multiplet-like peak intensities for Arg^{89} and Arg^{253} in this sample of ^2H-HCA II and obtain $P_{CH_2}=0.5$, $P_{CHD}=0.2$, and $P_{CD_2}=0.3$ as approximate values.

A similar ^{13}C multiplet-like pattern has been observed for Gln $^1H_{\varepsilon 21,22}/^{13}C_\gamma$ correlations in preliminary 2D $H_2(NCO)C_{\gamma/\beta}$ experiments where the ^1H-^{13}C scalar coupling has also not been refocused during the ^{13}C t_1 evolution period (data not shown). A detailed analysis of these peak lineshapes along the ^{13}C dimension reveals a 1:2:1 multiplet pattern, indicating that these particular carbons exist almost solely as the CH_2 moiety. This is in contrast to the arginine C_γ carbon, for which only $\sim 74\%$ of the total population exists as the CH_2 moiety. Examination of the glutamine and arginine biosynthetic pathway in *E. coli* reveals that the C_γ carbon in glutamic acid, glutamine, and arginine is derived from acetyl–CoA (Lehninger et al., 1993). Furthermore, the acetyl moiety in the acetyl–CoA complex is derived from the externally supplied ^{13}C-labeled acetate, which in our expression medium is fully protonated (Venters et al., 1995a). Glutamic acid is the precursor for both glutamine and arginine. Glutamic acid is converted to glutamine by amination in a single step, whereas a complex, multi-step process is required to convert glutamic acid to arginine. Because the glutamine C_γ carbon is observed to be $\sim 100\%$ protonated, we infer the same level of protonation for the glutamic acid C_γ. Our data indicate that at certain point(s) during the biosynthetic conversion of glutamic acid to arginine, there is some fractional abstraction of solvent ^2H atoms onto the C_γ carbon.

Although it is the glutamine and arginine C_γ carbons that retain a high level of specific protonation in our perdeuterated HCA II sample, glutamine (Fig. 3A) and arginine (Fig. 4B) C_γ correlations should suffer minimally in sensitivity because of the short ^{13}C t_1 evolution time (6.79 ms) that is employed. The t_1 evolution time, moreover, must be kept short both to minimize any line-broadening effects of homonuclear ^{13}C scalar coupling and to maximize the overall sensitivity of the experiment. The arginine C_γ correlations should be enhanced in sensitivity due to the deuteration of the arginine C_δ carbons. It is only the glutamine C_β correlations that may be reduced in intensity by the now apparently nonuniform perdeuteration of HCA II. We have attempted to assess the degree to which these latter correlations are compromised in sensitivity by making the following comparison: $R_{Asn}(\beta:\alpha) = [S/N(Asn\ C_\beta)] / [S/N(Asn\ C_\alpha)]$ versus $R_{Gln}(\gamma:\beta) = [S/N(Gln\ C_\gamma)] / [S/N(Gln\ C_\beta)]$. Four asparagine residues (Asn^{62}, Asn^{229}, Asn^{231} and Asn^{243}) and six glutamine residues (Gln^{53}, Gln^{103}, Gln^{135}, Gln^{136}, Gln^{157} and Gln^{254}) have been used in this comparison. Both $R_{Asn}(\beta:\alpha)$ and $R_{Gln}(\gamma:\beta)$ yield values of ~ 6, indicating that the glutamine $C_\gamma \rightarrow C_\beta$ transfer is no less efficient than the asparagine $C_\beta \rightarrow C_\alpha$ transfer for the chosen residues. The explanation for this may lie in the side-chain mobility of the chosen residues and the concomitant decrease in the glutamine C_γ relaxation rate under those circumstances.

The $\sim 100\%$ level of protonation at the glutamine C_γ carbon can nonetheless result in substantially weaker $^1H_{\varepsilon 21,22}/^{15}N_{\varepsilon 2}/^{13}C_\beta$ correlations in the 3D $H_2N(COC_{\gamma/\beta})C_{\beta/\alpha}$ spectrum for sufficiently immobile side chains, potentially complicating the assignment of the glutamine side-chain $^1H_N/^{15}N$ resonances. As an example, in Fig. 3B we have observed no C_β correlation for Gln^{221}. Due to the observation of strong NOE contacts between backbone H_N protons and the side-chain H_N protons of Gln^{221} (Venters et al., 1995b), the side chain of Gln^{221} is thought to be largely immobile. In this respect, the high level of protonation on the arginine C_γ carbon poses less of a problem because it is the deuterated C_δ carbon that is responsible for transferring magnetization to C_γ. Collectively, these considerations argue for the use of perdeuterated ^{13}C-labeled acetate in the protein expression medium, so that maximum sensitivity is achieved in assigning the side-chain $^1H_N/^{15}N$ resonances with the pulse sequences detailed in this study. With regard to NOE data on the current ^2H-HCA II sample, however, the high level of specificity in the residual protonation may prove advantageous in the effort to determine the global fold of HCA II.

Lysine residues

The final residue with an aliphatic side chain that offers yet additional exchangeable protons in a perdeuterated protein is lysine. We have constructed a nonrefocused version of the $H(N_{\varepsilon/\zeta})C_{\delta/\varepsilon}$ pulse sequence depicted in Fig. 1C, optimized for NH_3 groups, in order to detect $^1H_\zeta/^{13}C_\varepsilon$ correlations in lysine residues. No such correlations have been observed yet with this experiment (data not shown). Arginine $^1H_\varepsilon/^{13}C_\delta$ correlations, however, have been observed in this experiment. We therefore conclude that there are apparently no slowly exchanging side-chain lysine H_ζ amino protons in ^{2}H-HCA II. This conclusion is consistent with the crystal structure for HCA II (Liljas et al., 1972), which depicts the side chains of all 24 lysine residues protruding into the solvent.

Discussion

Correlations between side-chain ^{13}C, ^{15}N, and ^1H_N resonances for glutamine and asparagine residues in small protonated proteins have been previously observed both in the HC(CC)(CO)NH (Montelione et al., 1992), the HC(CC)NH (Lyons and Montelione, 1993; Lyons et al., 1993), and the HNCACB (Wittekind and Mueller, 1993) experiments. In perdeuterated proteins, however, the HC(CC)(CO)NH experiment must in general be replaced with the C(CC)(CO)NH experiment, in which magnetization starts on ^{13}C (Farmer II and Venters, 1995). Assuming that the side-chain amide protons experience negligible chemical exchange and negligible intergroup cross-relaxation during the δ_1, δ_2, δ_4, and t_1 delays (Fig. 1B), one would expect the experimental approaches described here for perdeuterated proteins to be significantly more sensitive than the C(CC)(CO)NH experiment.

To test this expectation, we have compared for the 19 chemical-shift resolved residues in HCA II that are i+1 to a glycine the S/N obtained in the HN(CO)CACB experiment (Yamazaki et al., 1994a) to that obtained in the C(CC)(CO)NH experiment. On average, the former yields a 2.2-fold greater S/N than the latter, with a range of 1.1 (Gly^{144}) to 4.1 (Gly^{25}). In this analysis, however, the backbone HN(CO)CA experiment would serve as a more representative model for the side-chain $H_2N(CO)C_{\gamma/\beta}$ experiment. Considering only scalar coupling transfer efficiencies, the HN(CO)CA should be at least twofold more sensitive than the HN(CO)CACB. In support hereof, it has been observed in protonated ^{13}C-/^{15}N-labeled apokedarcidin (Constantine et al., 1994) that for non-glycine C_α resonances, the HN(CO)CA experiment is ~1.9-fold more sensitive than the HN(CO)CACB (B.T. Farmer II, unpublished results). The C(CC)(CO)NH experiment, when applied to side-chain NH_2 groups, incurs an additional twofold loss in relative sensitivity during the $^{15}N \rightarrow {}^1H_N$ reverse INEPT transfer. The $H_2N(CO)C_{\gamma/\beta}$ experiment avoids this loss by not refocusing the $^{15}N_x{}^1H_z$ antiphase magnetization during δ_1. In total, the $H_2N(CO)C_{\gamma/\beta}$ experiment is estimated to be ~eightfold more sensitive than the C(CC)(CO)NH experiment in establishing side-chain ^{13}C to side-chain $^1H_N/^{15}N$ correlations in a perdeuterated protein.

Further benefits to the out-and-back approach can be envisioned on comparing the $H_2N(COC_{\gamma/\beta})C_{\beta/\alpha}$ experiment to the C(CC)(CO)NH one. In the latter, the maximum $C_\beta \rightarrow C_\gamma$ scalar coupling transfer efficiency for glutamine residues is calculated to be 45% for a CC-TOCSY transfer and 50% for a CC-COSY transfer. By comparison, the $C_\gamma \rightarrow C_\beta \rightarrow C_\gamma$ scalar coupling transfer efficiency in the out-and-back $H_2N(COC_{\gamma/\beta})C_{\beta/\alpha}$ experiment should be >95%. If specific residue types are considered, the situation may change for this particular ^{2}H-HCA II sample: magnetization in the C(CC)(CO)NH experiment could start on the H_γ protons for glutamine, thereby increasing the relative sensitivity of this approach for the glutamine C_γ side-chain correlations. This mechanism for sensitivity enhancement, however, is not available either to the asparagine C_α and C_β carbons or to the glutamine C_β carbons of ^{2}H-HCA II. We therefore believe that the pulse sequence depicted in Fig. 1B offers both the highest sensitivity and the greatest generality in the assignment of glutamine and asparagine side-chain amide groups, especially for proteins that are completely perdeuterated at aliphatic side-chain proton sites.

Several side-chain ^1H_N resonances in HCA II, e.g., Asn^{243} $H_{\delta 21}$ and Gln^{103} $H_{\varepsilon 22}$, experience ring-current shifts due to spatially proximal tryptophan residues. In particular, Asn^{243} $H_{\delta 21}$ is depicted in the X-ray structure of HCA II (Liljas et al., 1972) to be sandwiched between Trp^{97} and Trp^{244}. The possibility that such anomalously upfield-shifted ^1H_N resonances can occur poses a general problem for the recently developed water-flipback technique (Grzesiek and Bax, 1993; Kay et al., 1994). This technique relies on a selective 90° ^1H pulse, which follows the initial $^1H_N \rightarrow {}^{15}N$ INEPT transfer, to return the water magnetization to the ±z-axis without affecting any of the J-ordered ^1H_N spins. Unfortunately, any ^1H_N spin with a chemical shift sufficiently close to that of water will have its magnetization rotated into the transverse plane by this selective 90° ^1H pulse and subsequently destroyed by the ensuing purge gradients (Li and Montelione, 1995). Caution must therefore be exercised in the application of the water-flipback technique, especially if the range of protein ^1H_N chemical shifts has not yet been fully characterized.

In this study, we have determined the $^1H_N/^{15}N$ assignments both of side-chain amide groups for 9 of the 10 asparagine residues and 8 of the 11 glutamine residues and of side-chain ε amino groups for all seven arginine residues in ^{2}H-HCA II. We have also assigned the $^1H_\eta/^{15}N_\eta$ guanidino resonances for three arginine residues (Arg^{27}, Arg^{245}, and Arg^{253}) by through-bond correlations to the C_ζ carbon. The NMR results are consistent with

the crystal structure of HCA II, in that the side chains of only these three arginine residues are shown to be directed back into the protein core (Liljas et al., 1972). The side-chain ^1H_N / ^{15}N assignments obtained from this study are being used in conjunction with main-chain NH group assignments in the analysis of 3D ^{15}N-separated and 4D $^{15}N/^{15}N$-separated NOESY data obtained with long mixing times ($\tau_m > 150$ ms). A preliminary analysis of a 4D $^{15}N/^{15}N$-separated NOESY spectrum has already yielded several long-range NOEs between side-chain and backbone H_N protons (Venters et al., 1995b; Venters et al., unpublished results). The long-term goal of this effort is to calculate a global protein fold for HCA II using only ^1H_N-^1H_N NOE-derived distance restraints, an effort in which side-chain NH and NH_2 groups appear to play an important role (Venters et al., 1995b).

Acknowledgements

The Duke University NMR Center was established with grants from the NIH, NSF, and the North Carolina Biotechnology Center, which are gratefully acknowledged. B.T.F. would like to thank Drs. William Metzler and Luciano Mueller, both for their critical reading of the manuscript and for their valuable contributions.

References

Arrowsmith, C.H., Pachter, R., Altman, R.B., Iyer, S.B. and Jardetzky, O. (1990) *Biochemistry*, **29**, 6332–6341.

Bax, A., Clore, G.M. and Gronenborn, A.M. (1990) *J. Magn. Reson.*, **88**, 425–431.

Bax, A., Ikura, M., Kay, L.E. and Zhu, G. (1991) *J. Magn. Reson.*, **91**, 174–178.

Borders Jr., C.L., Broadwater, J.A., Bekeny, P.A., Salmon, J.E., Lee, A.S., Eldridge, A.M. and Pett, V.B. (1994) *Protein Sci.*, **3**, 541–548.

Bordo, D. and Argos, P. (1994) *J. Mol. Biol.*, **243**, 504–519.

Clowes, R.T., Boucher, W., Hardman, C.H., Domaille, P.J. and Laue, E.D. (1993) *J. Biomol. NMR*, **3**, 349–354.

Constantine, K.L., Colson, K.L., Wittekind, M., Friedrichs, M.S., Zein, N., Tuttle, J., Langley, D.R., Leet, J.E., Schroeder, D.R., Lam, K.S., Farmer II, B.T., Metzler, W.J., Bruccoleri, R.E. and Mueller, L. (1994) *Biochemistry*, **33**, 11438–11452.

Emsley, L. and Bodenhausen, G. (1987) *Chem. Phys. Lett.*, **165**, 469–472.

Farmer II, B.T. and Mueller, L. (1994) *J. Biomol. NMR*, **4**, 673–687.

Farmer II, B.T., Mueller, L., Nikonowicz, E.P. and Pardi, A. (1994) *J. Biomol. NMR*, **4**, 129–133.

Farmer II, B.T. and Venters, R.A. (1995) *J. Am. Chem. Soc.*, **117**, 4187–4188.

Grzesiek, S., Anglister, J. and Bax, A. (1993a) *J. Magn. Reson. Ser. B*, **101**, 114–119.

Grzesiek, S., Anglister, J., Ren, H. and Bax, A. (1993b) *J. Am. Chem. Soc.*, **115**, 4369–4370.

Grzesiek, S. and Bax, A. (1993) *J. Am. Chem. Soc.*, **115**, 12593–12594.

Kay, L.E., Ikura, M., Tschudin, R. and Bax, A. (1990) *J. Magn. Reson.*, **89**, 496–514.

Kay, L.E., Keifer, P. and Saarinen, T. (1992) *J. Am. Chem. Soc.*, **114**, 10663–10665.

Kay, L.E., Xu, G.-Y., Singer, A.U., Muhandiram, D.R. and Forman-Kay, J.D. (1993) *J. Magn. Reson. Ser. B*, **101**, 333–337.

Kay, L.E., Xu, G.Y. and Yamazaki, T. (1994) *J. Magn. Reson. Ser. A*, **109**, 129–134.

Lehninger, A.L., Nelson, D.L. and Cox, M.M. (1993) *Principles of Biochemistry*, 2nd ed., Worth Publishers, New York, NY.

LeMaster, D.M. and Richards, F.M. (1988) *Biochemistry*, **27**, 142–150.

LeMaster, D.M. (1990) *Q. Rev. Biophys.*, **23**, 133–174.

LeMaster, D.M. (1994) *Prog. NMR Spectrosc.*, **25**, 371–419.

Levitt, M.H. (1986) *Prog. NMR Spectrosc.*, **18**, 61–122.

Li, Y.-C. and Montelione, G.T. (1995) *Biochemistry*, **34**, 2408–2423.

Liljas, A., Kannan, K.K., Bergsten, P.-C., Waara, I., Fridborg, K., Strandberg, B., Carlbom, U., Jarup, L., Lovgren, S. and Petef, M. (1972) *Nature New Biol.*, **235**, 131–137.

Logan, T.M., Olejniczak, E.T., Xu, R.X. and Fesik, S.W. (1993) *J. Biomol. NMR*, **3**, 225–231.

Lyons, B.A. and Montelione, G.T. (1993) *J. Magn. Reson. Ser. B*, **101**, 206–209.

Lyons, B.A., Tashiro, M., Cedergren, L., Nilsson, B. and Montelione, G.T. (1993) *Biochemistry*, **32**, 7839–7845.

McCoy, M.A. and Mueller, L. (1992) *J. Magn. Reson.*, **98**, 674–679.

Montelione, G.T., Lyons, B.A., Emerson, S.D. and Tashiro, M. (1992) *J. Am. Chem. Soc.*, **114**, 10974–10975.

Patt, S.L. (1992) *J. Magn. Reson.*, **96**, 94–102.

Reisman, J., Jariel-Encontre, I., Hsu, V.L., Parello, J., Geiduschek, E.P. and Kearns, D.R. (1991) *J. Am. Chem. Soc.*, **113**, 2787–2789.

Schleucher, J., Schwendinger, M., Sattler, M., Schmidt, P., Schedletzky, O., Glaser, S.J., Sørensen, O.W. and Griesinger, C. (1994) *J. Biomol. NMR*, **4**, 301–306.

Shaka, A.J., Keeler, J., Frenkiel, T. and Freeman, R. (1983) *J. Magn. Reson.*, **52**, 335–338.

Torchia, D.A., Sparks, S.W. and Bax, A. (1988) *J. Am. Chem. Soc.*, **110**, 2320–2321.

Tsang, P., Wright, P.E. and Rance, M. (1990) *J. Am. Chem. Soc.*, **112**, 8183–8185.

Venters, R.A., Huang, C.-C., Farmer II, B.T., Trolard, R., Spicer, L.D. and Fierke, C.A. (1995a) *J. Biomol. NMR*, **5**, 339–344.

Venters, R.A., Metzler, W.J., Spicer, L.D., Mueller, L. and Farmer II, B.T. (1995b) *J. Am. Chem. Soc.*, **117**, 9592–9593.

Vis, H., Boelens, R., Mariani, M., Stroop, R., Vorgias, C.E., Wilson, K.S. and Kaptein, R. (1994) *Biochemistry*, **33**, 14858–14870.

Wesener, J.R., Moskau, D. and Guenther, H. (1985) *J. Am. Chem. Soc.*, **107**, 7307–7311.

Wittekind, M., Metzler, W.J. and Mueller, L. (1993) *J. Magn. Reson. Ser. B*, **101**, 214–217.

Wittekind, M. and Mueller, L. (1993) *J. Magn. Reson. Ser. B*, **101**, 201–205.

Yamazaki, T., Lee, W., Arrowsmith, C.H., Muhandiram, D.R. and Kay, L.E. (1994a) *J. Am. Chem. Soc.*, **116**, 11655–11666.

Yamazaki, T., Lee, W., Revington, M., Mattiello, D.L., Dahlquist, F.W., Arrowsmith, C.H. and Kay, L.E. (1994b) *J. Am. Chem. Soc.*, **116**, 6464–6465.

Yamazaki, T., Pascal, S.M., Singer, A.U., Forman-Kay, J.D. and Kay, L.E. (1995) *J. Am. Chem. Soc.*, **117**, 3556–3564.